JOURNAL OF MATERIALS SCIENCE 16 (1981) 2188–2192

Equilibria of hydroxyl defects in MgO

KWAN WAI CHENG, W. D. KINGERY
Ceramics Division, Department of Materials Science and Engineering, Massachusetts Institute of Technology, Cambridge, Massachusetts 02139, USA

Isochronal annealing studies were carried out on slow-cooled MgO single crystals. The annealing behaviour of the hydroxyl defects is consistent with a defect model in which brucite precipitates dissolve in MgO forming OH–V–OH defects with a heat of solution equal to 0.45 eV. These OH–V–OH defects further dissociate into V_{OH}^{-} defects and hydroxyl ions with a dissociation energy of 0.82 eV.

1. Introduction

The role of hydroxyl as a solute in MgO crystals is important in understanding properties such as the nature of irradiation damage [1]. Hydroxyl ions in magnesium oxide have characteristic absorption bands around the 3 μm infra-red region of the optical spectrum. Henderson and Sibley [2] studied the isochronal annealing characteristics of hydroxyl defects in MgO by infra-red (i.r.) spectroscopy. Starting with a slow-cooled sample, subsequently annealed at higher and higher temperatures, they found that the absorption peak heights changed with the annealing temperature; the 3296 cm^{-1} peak increased while the 3700 cm^{-1} peak decreased. It is generally accepted that the 3296 cm^{-1} and the 3700 cm^{-1} bands in MgO are related to the $(V_{Mg}''-OH_O^{\cdot})$ defect (commonly known as the V_{OH}^{-} centre [3])*, and to the brucite (or $Mg(OH)_2$) precipitates [5, 6], respectively. Henderson and Sibley attributed this behaviour to the solution of brucite in MgO creating V_{OH}^{-} centres. This paper examines the effect of annealing on the equilibria of the hydroxyl species.

2. Defect model

Brucite has a hexagonal structure which consists of a layer of Mg^{2+} ions in octahedral sites, another layer of hydroxyl ions, a layer of vacant octahedral sites, another layer of hydroxyl ions, etc. The decomposition of brucite to form MgO takes place along a coherent interface in which the {1 1 0} planes in brucite become {2 0 0} planes in MgO, and the {0 0 0 1} planes in brucite become {1 1 1} planes in MgO [7]. Fig. 1 shows the stacking sequence of ion layers in the ⟨1 1 1⟩ direction of MgO when the MgO lattice is interrupted by a thin slice of brucite. The degree of mismatch along the coherent planes I and II, is 4.5%.

Upon dissolution of one layer of brucite, the interface II in Fig. 1 moves to III. The OH^- layers A_2 and B_2 become the {1 1 1} planes of MgO with oxygen ions substituted by hydroxyl ions. The vacant layer of octahedral sites becomes a layer of vacant magnesium sites in MgO, with charge compensating the hydroxyl ions. The brucite molecules forming the layer (A_2IIIB_1) are responsible for the i.r. and Raman spectra [8] seen upon dissolution. The MgO lattice is doped with $(OH_O^{\cdot}-V_{Mg}''-OH_O^{\cdot})$ complexes† which form the layer $(B_2\square A_2)$. On further heating, this neutral complex breaks up into a V_{OH}^{-} centre and an isolated hydroxyl ion. For the precipitation of brucite in MgO, the reverse of this process would be expected.

Consider the reaction

$$Mg(OH)_2\,\mathrm{ppt} \rightarrow Mg_{Mg} + (OH_O^{\cdot}-V_{Mg}''-OH_O^{\cdot}). \qquad (1)$$

At equilibrium, the concentration of OH–V–OH centres can be expressed as

$$[\mathrm{OH{-}V{-}OH}] = \exp(\Delta S_2/k)\exp(-\Delta H_2/kT) \simeq \exp(-\Delta H_s/kT), \qquad (2)$$

---

*For the nomenclature of colour centres, refer to the review article by Sonder and Sibley [4]. The more common Kröger–Vink notation is also used throughout this article.

†This is referred to as the OH–V–OH centre.

0022–2461/81/082188–05$02.50/0

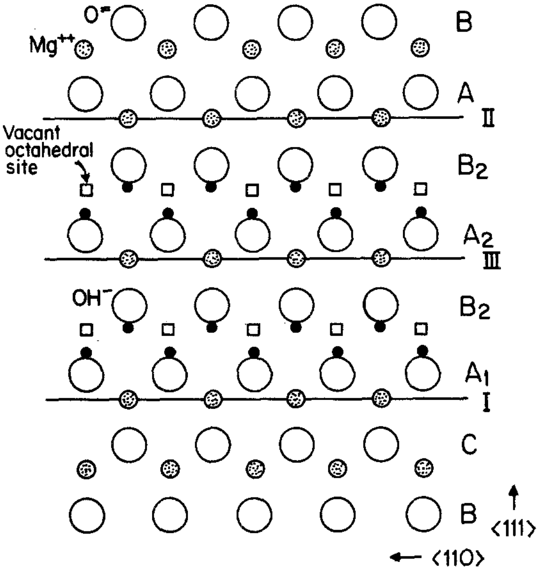

Figure 1 {111} plane of MgO interrupted by a layer of brucite. The A, B and C's are used for identifying the stacking sequences of the close-packed planes.

where ΔH_s is the heat of solution of brucite in MgO, ΔS_2 is the entropy change, T is temperature and k is a constant.

The OH–V–OH then separates into a V_{OH}^{-} centre and an isolated hydroxyl ion,

$$(\mathrm{OH{-}V{-}OH}) \rightarrow V_{\mathrm{OH}}^{-} + \mathrm{OH}_{\mathrm{O}}^{\cdot}, \qquad (3)$$

and

$$[\mathrm{OH}_{\mathrm{O}}^{\cdot}][V_{\mathrm{OH}}^{-}] = [\mathrm{OH{-}V{-}OH}]\exp(-\Delta H_d/kT), \qquad (4)$$

where ΔH_d is the dissociation energy of the OH–V–OH centre.

At higher temperatures, the V_{OH}^{-} formed by Equation 3 will split into a cation vacancy and a hydroxyl ion, i.e.

$$V_{\mathrm{OH}}^{-} \rightarrow V_{\mathrm{Mg}}'' + \mathrm{OH}_{\mathrm{O}}^{\cdot} \qquad (5)$$

and

$$[V_{\mathrm{Mg}}''][\mathrm{OH}_{\mathrm{O}}^{\cdot}] \simeq [V_{\mathrm{OH}}^{-}]\exp(-\Delta H_a/kT), \qquad (6)$$

where ΔH_a is the dissociation energy of the V_{OH}^{-} centre.

3. Experimental procedures

Nominally "pure" Norton* crystals and W & C Spicer* crystals, both containing a large hydroxyl impurity content, were used in the following procedures. Crystals were cleaved from optically clear, bubble-free regions. (Usually, crystals containing many hydroxyl ions are cloudy with hydrogen bubbles.) Impurity analyses of the crystals are tabulated in Table I. All these data, except for zirconium, were obtained by spectrographic analysis. Zirconium was determined by neutron-activation analysis [9].

Briggs [10] detected the possibility of precipitating hydrogen bubbles from the hydroxyl ions. The amount of hydrogen could be estimated by using the hydrogen pressure inside the bubbles and the volume fraction of the bubbles. In these crystals, the amount of hydrogen was estimated to be 10^{17} to $5 \times 10^{18}\ \mathrm{cm}^{-3}$.

Two slabs of Spicer crystals (total thickness = 2 mm) and three slabs of Norton crystals (total thickness = 2.42 mm) were used. Specimens were cleaved to form samples about a millimeter thick, and then chemically polished to a good optical finish in 85% phosphoric acid at 110° C.

The crystals were placed in a MgO crucible and annealed in air in a furnace which was controlled to ± 5° C. Each set of specimens was given the slow-cooling heat treatment shown in Table II prior to the isochronal study. This slow cooling procedure was designed to convert as much hydroxyl into brucite as possible. In the isochronal annealing study, the specimens were annealed for a fixed time (24 h for the Norton crystals and 1 h for the Spicer crystals) at the annealing temperature, and then quenched in liquid nitrogen. This procedure was repeated at progressively higher temperatures.

Infra-red absorption measurements were made after every heat treatment. The thin slabs were

TABLE I Impurity analyses of MgO crystals. Contents expressed as ppm by weight (taken from [8])

Element	Norton MgO	Spicer MgO
Ca	50	90
Al	70	50
Fe	50	< 20
Si	< 20	20
Cr	< 50	< 50
Mn	7	< 1
Ti; V; Zn	< 50	< 50
Co	< 20	< 20
Mo	< 10	< 10
Cd; Be; Sb	< 5	< 5
Cu; Ni; Sn	< 2	< 2
In; Bi; Pb	< 1	< 1
Ge; Ga	< 0.5	< 0.5
Zr	4	4

---

*The authors are indebted to Dr Alan Briggs of UKAERE, Harwell, UK for supplying these crystals. Samples cleaved from these same boules had been used in studies on hydrogen bubble formation in MgO [5, 8, 9].

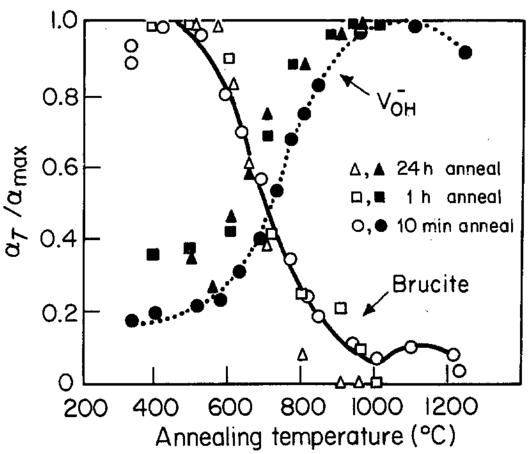

Figure 2 Plot of relative absorptivities against annealing temperatures.

TABLE II Cooling schedule prior to isochronal annealing

Stage	Process	
Norton crystals		
i	Held at:	900° C for 45 min
ii	Then cooled to:	800° C and held for 13 h
iii	Then cooled to:	640° C and held for 24 h
iv	Then cooled to:	550° C and held for 36 h
v	Then cooled to:	500° C and held for 11.5 h
vi	Then cooled to:	200° C in 8 h
Spicer crystals		
i	Held at:	900° C for 1 h
ii	Then cooled from:	900 to 600° C in 8 h
iii	Then held at:	600° C for 6 h
iv	Then cooled from:	600 to 200° C in 8 h

stacked together and mounted on a brass holder for measurements made on a Beckmann BK-12 and a Beckmann Acculab 10 spectrophotometer.

4. Results and discussion

When plotted against temperature, the relative absorptivities of the 3700 cm^{-1} brucite peak and the 3296 cm^{-1} V_{OH}^- peak yield curves similar to those obtained by Henderson and Sibley [2] (see Fig. 2). The results are tabulated in Table III.

As discussed above, OH–V–OH should form upon dissolution of brucite. The equilibrium reaction is described by Equation 2. The i.r. absorption peak of OH–V–OH is unknown; therefore, the concentration of OH–V–OH cannot be measured directly. However, since one mole of dissolved brucite gives one mole of OH–V–OH, the change in brucite concentration can be used to measure the change in OH–V–OH concentration. If the initial concentration of brucite in these slow-cooled crystals is taken as $[\text{brucite}]_{max}$, the OH–V–OH concentration at temperature T is

$$[\text{OH–V–OH}]_T \simeq [\text{brucite}]_{max} - [\text{brucite}]_T, \tag{7}$$

because the initial concentration of OH–V–OH is small.

The concentration of a defect centre is directly proportional to its optical absorptivity. Thus, Equation 2 can be written in the form

$$c(\alpha_{max} - \alpha_T) = \exp(-\Delta H_s/kT), \tag{8}$$

where c is a proportionality constant and the α's are the absorptivities of brucite at 3700 cm^{-1}. Plotted in this way (Fig. 3) the data give a straight line with an activation energy equal to 0.45 eV at temperatures between 600 and 850° C.

For the dissociation of OH–V–OH into V_{OH}^- and $OH_O^\cdot$, the equilibrium is expressed as Equation 4, but the optical absorption band of $OH_O^\cdot$ is unknown; therefore, the concentration of the OH–V–OH and of the $OH_O^\cdot$ cannot be measured directly. However, since one mole of OH–V–OH dissociated into one mole of V_{OH}^- and one mole of $OH_O^\cdot$, the change in the concentration of V_{OH}^- can be used to measure the change in OH–V–OH and $OH_O^\cdot$ concentrations.

Equation 4 can be written as

$$K = \frac{[V_{OH}^-]_T^2}{[V_{OH}^-]_{max} - [V_{OH}^-]_T}, \tag{9}$$

where K is the equilibrium constant.

Since the concentration of the defect is directly proportional to its optical absorptivity, Equation 9 can also be expressed as

$$K' = \frac{\alpha_T^2}{\alpha_{max} - \alpha_T}, \tag{10}$$

where the α's are the absorptivities of V_{OH}^- at 3296 cm^{-1}. Data are plotted this way in Fig. 4, where activation energies in the range 1.13 to 1.42 eV, with an average value of 1.27 eV, are obtained. The data fit Equation 10 for over two orders of magnitude. Since OH–V–OH is formed from the dissolution of brucite, the experimental activation energy includes the heat of solution of brucite. Thus, the dissociation energy of OH–V–OH is estimated to be 1.27 minus 0.45 or 0.82 eV.

The dissociation energy of OH–V–OH can be

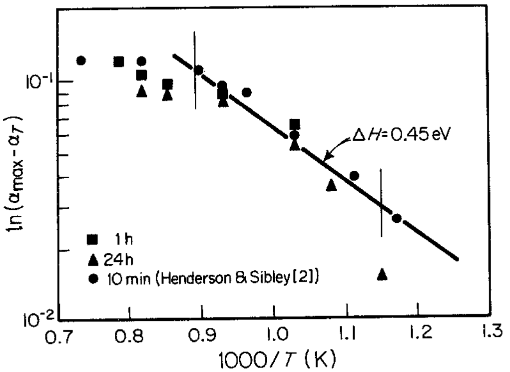

Figure 3 Plot of the brucite absorptivity using Equation 8. The vertical bars show the region in which the data in Fig. 4 fitted Equation 10 very well.

estimated by a simple coulombic calculation. Using a dielectric constant of 9.8 [11] and assuming that the $OH^{\bullet}_O$ and V''_{Mg} are point charges, a dissociation energy of 1.05 eV results. The experimental value of 0.82 eV is in reasonable accord with this simple calculation, as has been found for other point defect association energies in MgO [12].

Attempts to continue this isochronal anneal at temperatures above 1000° C results in an irreversible loss of hydroxyl defects. The rate of loss is diffusion-controlled [13].

Chen and Sibley [14] studied the isochronal annealing behaviour of V^- centres in slow-cooled MgO crystals. Crawford [15] analysed their results with an equation similar to Equation 9 here and obtained an activation energy of 1.44 eV. This is no surprise as Chen *et al.* [1] pointed out that V_{OH}^- centres are precursors to V^- centre formation; their results are close to those of the present study.

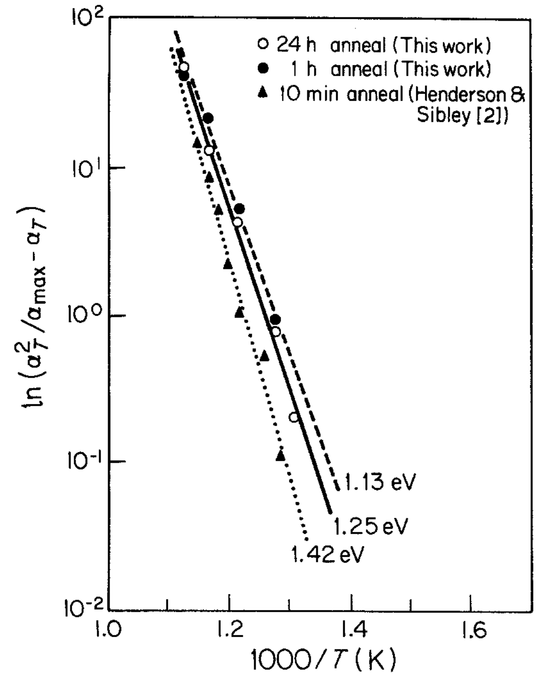

Figure 4 Plot of the V_{OH}^- absorptivity using Equation 10.

The influence of impurities appears in the presence of a weak 3310 cm^{-1} absorption band which belongs to the OH–V–I centre, a trivalent

TABLE III Absorptivities of the brucite and V_{OH}^- bands for the two sets of crystals at different temperatures

T (° C)	Norton crystals; 24 h anneals; total thickness = 2.42 mm		Spicer crystals; 1 h anneals; total thickness = 2 mm	
	α_T (3700)* (per cm)	α_T (3296)† (per cm)	α_T (3700)* (per cm)	α_T (3296)† (per cm)
400	—	—	1.20	1.18
450	—	—	—	—
500	0.89	0.69	1.14	1.22
550	0.87	0.55	—	—
600	0.74	0.92	1.10	1.33
650	0.54	1.16	—	—
700	0.35	1.50	0.54	2.25
750	—	—	—	—
800	0.09	1.76	0.32	2.84
850	—	—	—	—
900	0	1.92	0.25	3.00
950	0	2.0	0.13	3.17
1000	—	—	—	3.21

*The absorptivity at temperature T at 3700 cm^{-1}.
†The absorptivity at temperature T at 3296 cm^{-1}.

impurity bonded to a V_{OH}^- centre [2], which was not studied.

References

1. Y. CHEN, M. M. ABRAHAM, L. C. TEMPLETON and W. P. UNRUH, *Phys. Rev. B.* **11** (1975) 881.
2. B. HENDERSON and W. A. SIBLEY, *J. Chem. Phys.* **55** (1971) 1276.
3. P. W. KIRKLIN, P. AUZINS and J. E. WERTZ, *J. Phys. Chem. Sol.* **26** (1965) 1067.
4. E. SONDER and W. A. SIBLEY, in "Point Defects in Solids", Vol. 1. Edited by J. H. Crawford, Jr and L. M. Shifkin, (Plenum Press, New York, 1972) p. 208.
5. A. BRIGGS, *J. Mater. Sci.* **10** (1975) 729.
6. *Idem, ibid.* **12** (1977) 637.
7. R. S. GORDON and W. D. KINGERY, *J. Amer. Ceram. Soc.* **49** (1966) 654.
8. R. A. BUCHANAN, H. H. CASPERS and J. MURPHY, *Applied Optics* **2** (1963) 1147.
9. A. BRIGGS, PhD thesis, University of Bradford.
10. *Idem, J. Mater. Sci.* **10** (1975) 737.
11. E. BURSTEIN, in "Phonons and Phonon Interactions", edited by T. A. Bak (Benjamin, New York, 1964) p. 276.
12. W. H. GOURDIN and W. D. KINGERY, *J. Mater. Sci.* **14** (1979) 2074.
13. K. W. CHENG, ScD thesis, MIT, 1981.
14. Y. CHEN and W. A. SIBLEY, *Phys. Rev.* **154** (1967) 842.
15. J. H. CRAWFORD, Jr, *Crystal Lattice Defects* **1** (1970) 357.

Received 20 October 1980 and accepted 2 February 1981.